CHARACTERISATION OF FATIGUE MICROMECHANISMS IN TOUGHENED CARBON FIBER-POLYMER COMPOSITES USING SYNCHROTRON RADIATION COMPUTED TOMOGRAPHY

S. C. Garcea[a*], I. Sinclair[a], S. M. Spearing[a]

[a]*Materials Research Group, Faculty of Engineering and the Environment, University of Southampton, Southampton, United Kingdom*
**scg1a09@soton.ac.uk*

Keywords: Carbon/epoxy, Fatigue, Toughening systems, Synchrotron radiation computed tomography

Abstract

Toughening micromechanisms in double-notch tension cross-ply carbon/epoxy coupons have been investigated using synchrotron radiation computed tomography. The fatigue behaviour of toughened and untoughened systems has been compared; highlighting similarities and differences in terms of damage initiation and propagation. Damage does not propagate evenly for the toughened systems: the presence of resin rich regions constrains crack propagation, retarding damage growth. In contrast, the untoughened system is characterized by more uniform crack propagation. The particle-toughened system shows a higher propensity for crack deflection and the creation of bridging ligaments along the crack wake, due to particle debonding events, which lead to discontinuous microcrack formation. The principal effect of fatigue loading is the degradation of bridging ligaments in the crack wake.

1. Introduction

Carbon fibre reinforced polymer (CFRP) composites are a potent weight reducing structural technology. In addition their resistance to fatigue and corrosion makes these materials of particular interest for aerospace applications. However, their fatigue resistance is often not fully exploited in design, due to the difficulty of predicting fatigue life and it presents the barrier to the adoption of damage tolerant design approaches. Damage processes in CFRPs have been extensively investigated using different approaches, [1-7]; however, overly conservative and empirical design methods remain standard in engineering practice.
Thermosetting composites exhibit high strength and stiffness, but offer inadequate impact damage resistance and tolerance. Addressing the improvement of the fracture toughness of thermosetting net resins has been a key focus of material development. Various solutions have been investigated: insertion of rubber particles [8-9], thermoplastic particles [10], and rigid fillers [11]; varying particle dimension from nano to micro scale [12]. To date, several approaches to toughening have been developed to a sufficient level of maturity that they are employed in service for CFRPs for aerospace applications; however, the underpinning micromechanisms have not been widely investigated. Limited research is available in the literature as to the toughening micromechanisms in composites [13-16], and to the authors' knowledge there has not been any work to understand the consequence of fatigue loading on

the effectiveness of toughening strategies. Consequently, the effectiveness and optimization of specific toughening systems in terms of damage reduction and fracture toughness remains a relatively empirical process.
Previous studies have been conducted on carbon fibre/epoxy laminated composites using X-ray computed tomography, demonstrating the potential of this technique for assessing damage micromechanisms for small coupons subjected to quasi-static [17], impact [15,16], and fatigue loading [18]. The detail and the accuracy obtained using a resolution on the order of 1 μm has been shown to be appropriate for capturing both primary damage events (such as ply cracking), along with key local events such as the decohesion of toughening particles or fibres, facilitating correlation with primary microstructural features such as the ply structure and the presence of resin-rich and fibre-rich regions.
The present work represents the first use of *in situ* SRCT imaging to understand the micromechanisms operating in toughened and untoughened composite systems subjected to fatigue loading. The comparison of damage initiation/propagation for these three different material configurations provides key insights as to the effect of fatigue on the micromechanisms of damage resistance in toughened composite systems.

2. Materials and method

2.1 Materials

Three carbon/epoxy material systems have been used in the present work: two toughened systems; one containing thermoplastic toughening particles (M21/T700), the other utilizing a homogeneous, intrinsically toughened matrix (8852/IM7), and an untoughened system (3501-6/IM7). All systems contain intermediate modulus carbon fibres. For all three materials a cross-ply lay up was used, however, the sacking sequence was slightly different between the particle-toughened system, which has a $[90/0]_s$ layup, with double-thickness (250 μm) plies and the other two systems which have standard, (125 μm) thickness individual plies in a $[90/0]_{2s}$ layup. In all three materials the nominal overall thickness was maintained at ~1 mm.

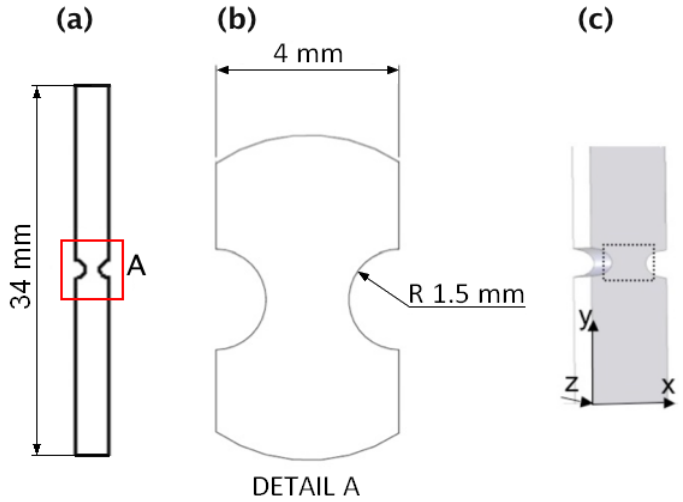

Figure 1 – Specimen used for *in situ* fatigue tests: geometry and dimensions, (b) of the notch region, (c) schematic of the reference coordinate system used.

Materials were laid up and auto-clave cured as flat plates using a standard aerospace cure cycle. Rectangular coupons containing two semi-circular notches of radius 1.5 mm were introduced by water jet cutting, leaving a nominal central cross-section between the notches of 1 mm. The geometry and dimensions of the specimens used are shown in Figure 1. The

need to have a length of 34 mm, is only associated with the requirement to fit the coupons in the fatigue device to perform the *in situ* experiments.

Material	UTS (MPa)	C_v
M21/T700	918	0.03
8852/IM7	1271	0.12
3501-6/IM7	1419	0.07

Table 1 – Ultimate tensile failure strength for material systems considered [19].

The average ultimate tensile failure strength (UTS) for each material system has been evaluated in previous studies [19], and is calculated based on the failure load and the net cross-sectional area between the notches. Values are reported in Table 1, where C_v represents the coefficient of variation. The tendency for the specimens to split and delaminate extensively before failure justifies the use of the net section to calculate the nominal UTS.

2.2 Fatigue tests and SRCT scan procedure

Tensile fatigue tests with a peak load of 50% of the tensile failure strength were performed using a load ratio of R=0.1, and a frequency of 5 Hz. Fatigue cycling was initially carried out using a standard servo-hydraulic load frame to apply 700 load cycles. After these load cycles were applied, the coupons were scanned at the Swiss Light Source (SLS), TOMCAT-X02DA Beamline, Paul Scherrer Institut, Villigen, Switzerland. After this first scan, each specimen was placed in the load frame and an additional 100 cycles were applied, then the specimen imaged again. The particular focus of this work is to determine the evolution of the crack tip process zone and the corresponding damage events (e.g. microcracking ahead of the main crack) at the length-scale of individual microstructural features (e.g. toughening particles, fibres). The high resolution and full-field imaging afforded by SRCT allows detailed observations to be made with relatively few cycles applied.
Scans were conducted placing specimens at a distance of ~22 mm from the detector to allow a degree of phase contrast to be obtained. During each tomographic scan, 1500 projections were collected through the rotation of 180º. The beam energy was 19 KeV, and an isotropic voxel resolution of 0.69 μm was used.

3. Results

3.1 Particle toughened system

The particle-toughened M21/T700 system showed highly non-uniform growth of the fatigue crack front, exhibiting zones of retarded crack growth corresponding to resin rich regions [18]. Detailed imaging, as shown in Figure 2, has been focused on these regions with the aim of understanding the mechanisms that influence overall damage propagation. The initial process of damage propagation at the nominal crack tip is represented by particle debonding (Figure 2(b), highlighted ‘A’), which results in the creation of bridging ligaments along the crack wake. The process is distributed over a length of approximately 1 mm around the nominal crack tip. Comparison of Figure 2(a) and (b) reveals that the majority of the crack path (>50%) may be made up of discontinuous cracks on the order of 10’s of micrometres length, as opposed to sustained propagation of a dominant crack tip.

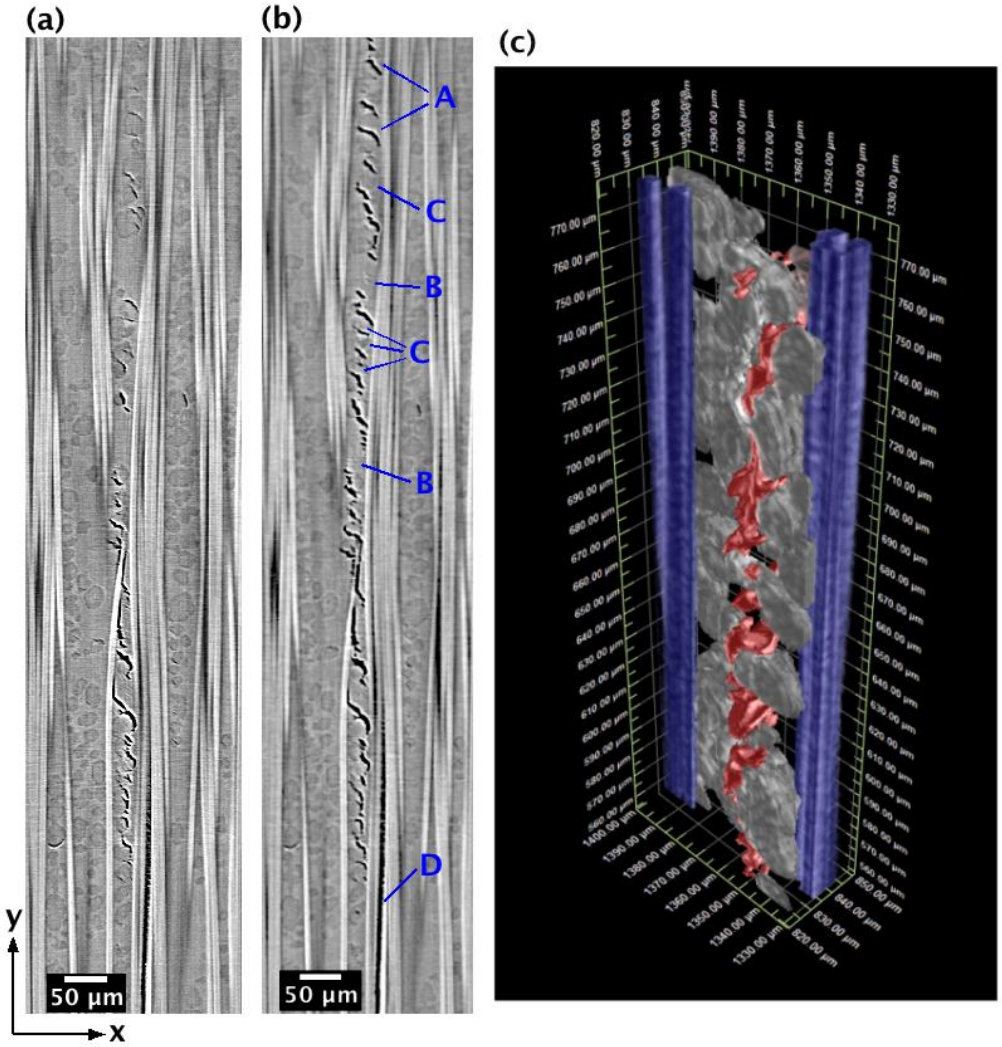

Figure 2 - Split growth propagation in M21/T700 within the resin rich region for a peak load of 50% UTS: 700 cycles (a) and 800 cycles (b). Damage development is affected by the microstructure: particle debonding at the crack tip [A], bridging ligaments by resin [B] and by particles [C], damage propagation at the fibre/matrix interface [D], and (c) 3D rendering of a region within the resin rich zone: 0˚ ply split (red) between toughening particles (grey) and fibres oriented along the loading direction (blue).

The periodicity of microcracking is clearly largely defined by the particle size and separation distances, see Figure 2(c). In particular, crack bridging ligaments consist of resin between particles (Figure 2(b), highlighted 'B') and/or by particles located in the direction of 0˚ ply split propagation (Figure 2(b), highlighted 'C').

The presence of particles promotes crack deflection, increasing the crack path tortuosity and the crack surface roughness. Figure 2(b) shows clearly the difference between the split growth propagation along the interface fibre/matrix (highlighted 'D'), which appears smooth and straight, versus the damage development in the resin rich region, characterized by significant crack deflection. These evaluations show that the resin rich regions tend to restrict damage propagation. This is consistent with observations at ply interfaces, which contain the majority of toughening particles: relatively extensive delamination has been detected at interfaces with a thin resin rich region.

Isolated, single fibre breaks have been detected adjacent to 0˚ ply splits, mainly associated with misaligned fibres and with the occasional development of cracks along fibre interfaces, as shown in Figure 3. Figure 3(a) shows a cross-section parallel to the loading direction of split growth at the fibre/matrix interface after 700 cycles at a peak load of 50% UTS.

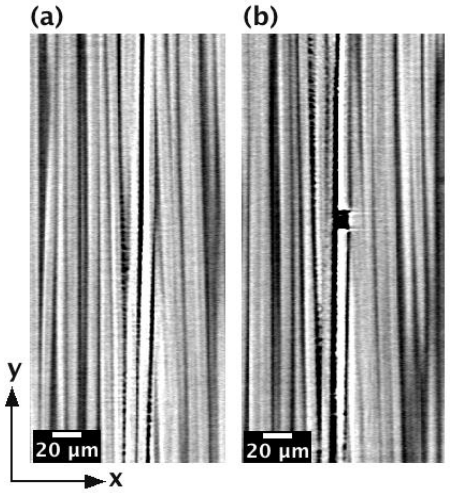

Figure 3 – 0º ply split development in M21/T700 at the fibre/matrix interface for 50% UTS: 700 cycles (a) with consequently fibre failure in correspondence of 800 cycles (b).

The split has propagated, causing fibre debonding on both sides. As debonding propagates at both fibre/matrix interfaces, the fibre is increasingly detached from the surrounding matrix, reducing its load bearing capacity, ultimately resulting in failure, Figure 3(b).

3.2 Untoughened system

The untoughened system exhibits fewer and smaller resin-rich regions, especially within each individual ply. This microstructure clearly affects damage initiation, which occurs preferentially at the fibre/matrix interfaces (rather than at toughening particles) for both 0˚ ply splits and delaminations, as shown in Figure 4. 0˚ ply splits propagate as a continuous crack along the fibre interface, in a similar manner to that observed within high fibre volume fraction zones of the particle-toughened system.

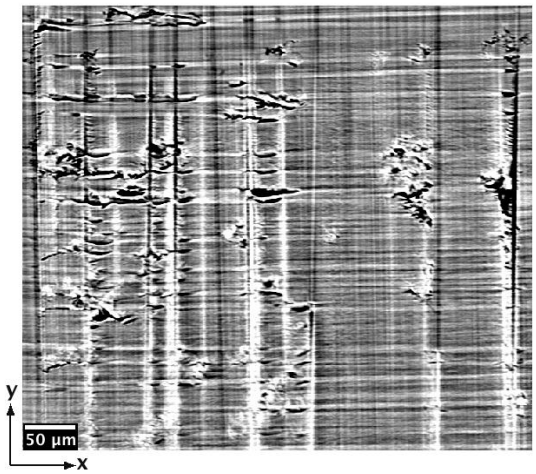

Figure 4 - Delamination sites for the untoughened material system (3501-6/IM7) after 700 cycles at a load of 50% UTS.

Fatigue loading of the untoughened system generated a higher number of fibres breaks for a given load level and number of cycles, see Figure 5, where fibre breaks are highlighted with red circles. Fibre breaks are principally located in the region between the split paths within the 0˚ ply, (Figure 5, splits are highlighted blue), and at ply interfaces, where delamination has occurred. At this stage it is difficult to identify the mechanism linking delamination and fibre

breaks, however, experimental observations have shown that no fibre breaks are observed at interfaces that do not exhibit delamination.

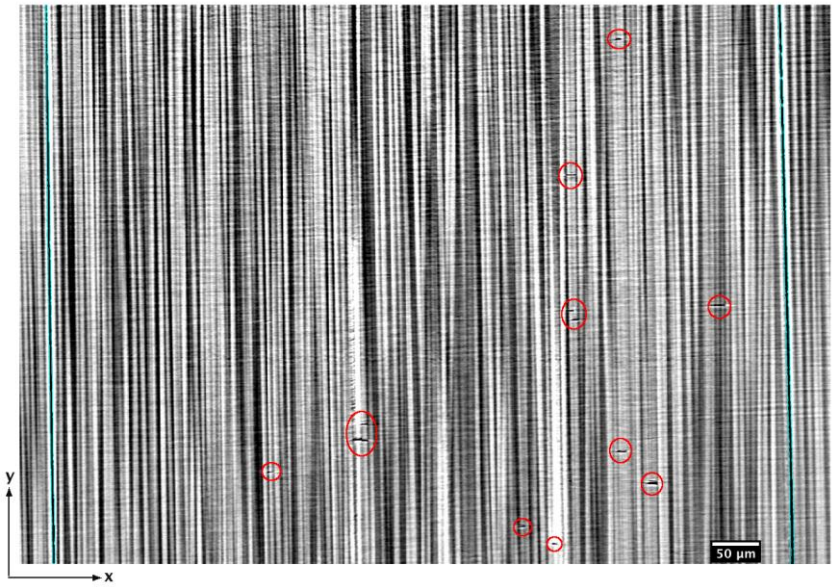

Figure 5 - Fibre breaks (highlighted with the red circle) in 3501-6/IM7 in the region between the two 0º ply splits (in blue).

3.3 Intrinsically toughened matrix system

The intrinsically toughened matrix (8552) results in fatigue behaviour that is intermediate to the untoughened and particle toughened systems: intralaminar damage initiates in high fibre volume fraction regions as fibre debonding and propagates in a relatively straight/simple manner (Figure 6(a)), whereas failure in resin rich regions occurs via small microcracks originating at the fibre/matrix interface, Figure 6(b).

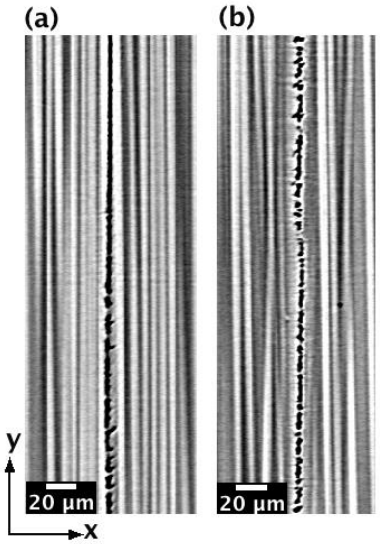

Figure 6 – 0º ply split growth in the 8552/IM7 in the fibre packed region (a), and in correspondence of fibres surrounded by resin (b).

The resin remaining between microcracks forms bridging ligaments, which are smaller than those in the particle-toughened system, Figure 6(b). In addition, the segmentation of the 0º ply

splits has shown, that as for the particle-toughened material, the resin rich regions retardate damage growth.
Isolated fibre breaks have been detected within the 0º plies in the region between the splits, however, no relation with other damage modes has been found.

4. Discussion

The experimental observations conducted in this work have showed that the fatigue damage micromechanisms depends on microstructure, leading to a different behaviour between toughened and untoughened systems. The key mechanism identified for the particle-toughened system is the degradation during cycling of bridging ligaments introduced by particles along the crack wake. Previous results found by Bull *et al*. considering composites subjected to impact damage [16] showed that the tendency to form bridging ligaments correlates strongly with the resulting impact damage resistance. This suggests that fatigue may be particularly detrimental to structures that have already sustained damage due to impact. It is as yet unclear if toughening strategies alter the overall fatigue performance of undamaged structures relative to the untoughened materials. Based on these considerations, the next step in the present work will be to evaluate the effectiveness of the toughening micro-mechanisms in terms of fatigue damage tolerance.

5. Conclusions

In situ SRCT has been used to investigate the fatigue behaviour of toughened and untoughened CFRP composite material systems. Results showed that damage initiation/propagation is related to the local microstructure. Toughening systems exhibit bridging ligaments along the crack wake, whereas for the untoughened system cracks appeared to be continuous and smooth. The toughened systems sustained a few isolated fibre breaks during fatigue loading, whereas the untoughened system showed a higher number of fibre breaks within the 0º plies, and within the regions close to the delaminations. Overall the use of SRCT has revealed details of fatigue micromechanisms that have hitherto been impossible to identify, further illustrating its power as a tool for investigating the micromechanics of composite materials.

Acknowledgements

The authors would like to acknowledge funding from AFOSR-EOARD, grant 113040, Programme Monitor: Lt. Col. Randall Pollak. Also funding from EPSRC, grant EP/H1506X/1. The authors are grateful to the Swiss Light Synchrotron Radiation for access to TOMCAT-X02DA beamline, and to the assistance Dr. Sarah Irvine. Materials were supplied via Airbus SAS and Teledyne Technologies Incorporated.

References

[1] S.M. Spearing, P.W.R. Beaumont and M.F. Ashby. Fatigue damage mechanics of composite materials. II: a damage growth model. *Composites Science and Technology*, Vol. 44, No. 2, pp. 169-177, 1992.
[2] S.M. Spearing and P.W.R. Beaumont. Fatigue damage mechanics of composite materials Part III: prediction of post-fatigue strength. *Composites Science and Technology*, Vol. 44, No. 4, pp. 299-307, 1992.

[3] S. Subramanian, K.L. Reifsnider and W.W. Stinchcomb. A cumulative damage model to predict the fatigue life of composite laminates including the effect of a fibre-matrix interphase. *International Journal of Fatigue*, Vol. 17, No. 5, pp. 343-351, 1995.

[4] C. Koimtzoglou, V. Kostopoulos and C. Galiotis. Micromechanics of reinforcement and damage initiation in carbon fibre/epoxy composites under fatigue loading. *Composites Part A: Applied Science and Manufacturing*, Vol. 32, No. 3, pp. 457-471, 2001.

[5] Y.A. Dzenis. Cycle-based analysis of damage and failure in advanced composite under fatigue 2. Stochastic mesomechanics modeling. *International Journal of Fatigue*, Vol. 25, No. 6, pp. 511-520, 2003.

[6] J.R. Gregory and S.M. Spearing. Constituent and composite quasi-static and fatigue fracture experiments. *Composites Part A: Applied Science and Manufacturing*, Vol. 36, No. 5, pp. 665-674, 2005.

[7] R. Talreja. Damage and fatigue in composites – a personal account. *Composites Science and Technology*, Vol. 68, No. 13, pp. 2581-2591, 2008.

[8] A.F. Yee and R.A Pearson. Toughening mechanisms in elastomer-modifies epoxies, Part 1 Mechanical studies. *Journal of Materials Science*, Vol. 21, pp. 2462-2474, 1986.

[9] H.R. Azimi, R.A. Pearson, R.W. Hertzberg. Fatigue of rubber-modified epoxies: effect of particle size and volume fraction. *Journal of Materials Science*, Vol. 31, pp. 3777-3789, 1996.

[10] R.A. Pearson, A.F. Yee. Influence of particle size and particle size distribution on toughening mechanisms in rubber-modified epoxies. *Journal of Materials Science*, Vol. 26, pp. 3828-3844, 1991.

[11] J. Spanoudakis, R.J. Young. Crack propagation in a glass particle-filled epoxy resin, Part 1 Effect of particle volume fraction and size. *Journal of Materials Science*, Vol. 19, pp. 473-486, 1984.

[12] S.-Y. Fu, X.-Q. Feng, B. Lauke, Y.-W. Mai. Effect of particle size, particle/matrix interface adhesion and particle loading on mechanical properties of particulate-polymer composites. *Composites Part B: engineering*, Vol. 39, pp. 93-961, 2008.

[13] J. Kim, C Baillie, J. Poh, Y-W. Mai. Fracture toughness of CFRP with modified epoxy resin matrices. *Composites Science and Technology*, Vol. 43, pp. 283-297, 1992.

[14] F. Gao, G. Jiao, Z. Lu, R. Ning. Mode II delamination and damage resistance of carbon/epoxy composite laminates interleaved with thermoplastic particles. *Journal of Composite Materials*, Vol. 41. No 1, pp. 111-123, 2007.

[15] D.J. Bull, S.M. Spearing, I. Sinclair, L. Helfen. Three-dimensional assessment of low velocity impact damage in particle toughened composite laminates using micro-focus X-ray computed tomography and synchrotron radiation laminography. *Composites: Part A*, Vol. 52, pp. 62-69, 2013.

[16] D.J. Bull, A.E. Scott, S.M. Spearing, I. Sinclair. The influence of toughening-particles in CFRPs on low velocity impact resistance performance. *Composites: Part A*, Vol. 58, pp. 47-55, 2014.

[17] A.E. Scott, M. Mavrogordato, P. Wright, I. Sinclair, S.M. Spearing. In situ fibre fracture measurement in carbon-epoxy laminates using high resolution computed tomography. *Composites Science and Technology*, Vol. 71, pp. 1471-1477, 2011.

[18] S.C. Garcea, M.N. Mavrogordato, A.E. Scott, I. Sinclair, S.M. Spearing. Synchrotron computed tomography of fatigue micromechanisms in CFRP. *The 19th International Conference on Composite Materials*, Montreal, 2013.

[19] P.M. Wright. Investigation of damage in laminated carbon fibre composites using high resolution computed tomography, *Ph.D. Thesis*, pp. 41, 2011.